Effect of submicron holes on the vortex dynamics of a superconducting microbridge

J. Bentner,[1] D. Babić,[2,*] C. Sürgers,[3] and C. Strunk[1]
[1]*Institut für experimentelle und angewandte Physik, Universität Regensburg, D-93025 Regensburg, Germany*
[2]*Department of Physics, Faculty of Science, University of Zagreb, Bijenička 32, HR-10000 Zagreb, Croatia*
[3]*Physikalisches Institut and DFG Center for Functional Nanostructures (CFN), Universität Karlsruhe, D-76128 Karlsruhe, Germany*
(Received 13 April 2004; revised manuscript received 30 June 2004; published 17 November 2004)

We measured and compared the electric field vs current density characteristics in the vortex state of two amorphous $Nb_{0.7}Ge_{0.3}$ microbridges, with and without a line of submicron holes patterned along the sample axis. The power dissipation in the perforated sample exhibits a crossover, being reduced at temperatures well below the superconducting transition temperature T_c and unexpectedly enhanced close to T_c. At low temperatures the holes are efficient artificial pinning centers and reduce the average vortex velocity. We argue that the dissipation enhancement close to T_c is a consequence of a combination of the weakened pinning by the holes and an inhomogeneous driving-current distribution in their vicinity, which results in an increased average vortex velocity as well as in a channeling of the vortex motion through the holes.

DOI: 10.1103/PhysRevB.70.184516 PACS number(s): 74.78.Na, 74.40.+k, 74.25.Qt

I. INTRODUCTION

The rapid development of nanostructuring methods in the last decade has enabled highly precise fabrication of artificial pinning centers (APC's) for vortices in superconductors. It has already been proved that pointlike inclusions in a superconducting film, such as perforating holes,[1,2] structural defects,[3] and magnetic dots,[4] can pin vortices. A regular two-dimensional array of APC's stabilizes the vortex lattice against external driving forces, and results also in commensurability effects which scale with a matching magnetic field $B_M = \phi_0/S$, where S is the area of the array unit cell and ϕ_0 the magnetic flux quantum.[1] At a magnetic field $B > B_M$ vortices fill in the interstitial positions as well, where they are subject to intrinsic pinning originating from the structural defects. In a certain B range above B_M they may even form a commensurate multiple-flux-quanta lattice, as revealed from magnetization measurements.[2] A less symmetrical APC landscape, such as a rectangular array[5] or a set of parallel continuous lines of a magnetic material,[6] introduces anisotropies to the vortex transport. So far the effects of APC's have been found to be important at temperatures T rather close to T_c, typically at reduced temperatures $t = T/T_c > 0.9$, whereas at lower temperatures the intrinsic pinning dominated. Moreover, APC's invariably decreased the dissipation, apart from in a recent report.[7]

The simplest APC is a small perforating hole in a superconductor, having magnetic permeability larger than its diamagnetic surroundings. The most efficient pinning is obtained if the hole diameter is comparable to the magnetic-field penetration depth λ rather than the coherence length ξ, as one may expect at first sight. This was predicted by virtue of the Ginzburg-Landau (GL) theory for a single hole[8] and observed experimentally for two-dimensional arrays of holes.[9] The relevance of λ for the artificial pinning potential is a consequence of the comparatively small supercurrent kinetic energy required for preserving the flux-quantization condition around a hole not smaller than λ.

Local interactions of vortices with holes in the presence of a driving current have not yet been studied in detail experimentally. These go beyond the cited matching phenomena and are important for understanding the function of holes in an arbitrary arrangement, which may have implications for possible design of future devices based on manipulation of artificially pinned vortices. In this report we present such an investigation facilitated by arranging the holes in a line centred along the main axis of a superconducting microbridge [lower inset to Fig. 1(a)], which eliminates the matching phenomena but still provides a sufficient signal arising from the presence of the holes. In addition, we have minimized the influence of the intrinsic pinning by using the amorphous superconductor $Nb_{0.7}Ge_{0.3}$, which is known for its very low background pinning.[10,11] Another property of this material is its relatively large λ and small superconducting condensation energy U_c. This results in weak vortex-vortex correlations, the strength of which decreases with decreasing U_c and λ^{-2}, and thus permits using simplified, essentially single-vortex models in analyzing the vortex-motion phenomena.

The vortex motion was detected by recording the electric field vs current density characteristics $E(J)$ at constant (B,T), in three different temperature regimes, over a wide range of applied currents and B up to the upper critical magnetic field B_{c2}. Close to T_c we observed a clear increase of the power dissipation by the holes over the whole range of B and J. This result can be explained plausibly by taking into account a local enhancement of the vortex driving force due to a spatial modulation of the driving-current density around the holes. To our knowledge such current-modulation effects have so far been disregarded in the interpretation of previous experiments carried out on perforated superconductors. Well below T_c the holes pin the vortices and reduce the dissipation, which shows that their usefulness as APC's may extend to low temperatures if the intrinsic pinning is weak. Our results imply that the interplay of hole pinning and inhomogeneous current drive determines whether the holes enhance or reduce the dissipation in the vortex transport.

II. EXPERIMENT AND RESULTS

Two 210 μm long, 5 μm wide, and 20 nm thick microbridges between two large contact pads were sputtered onto

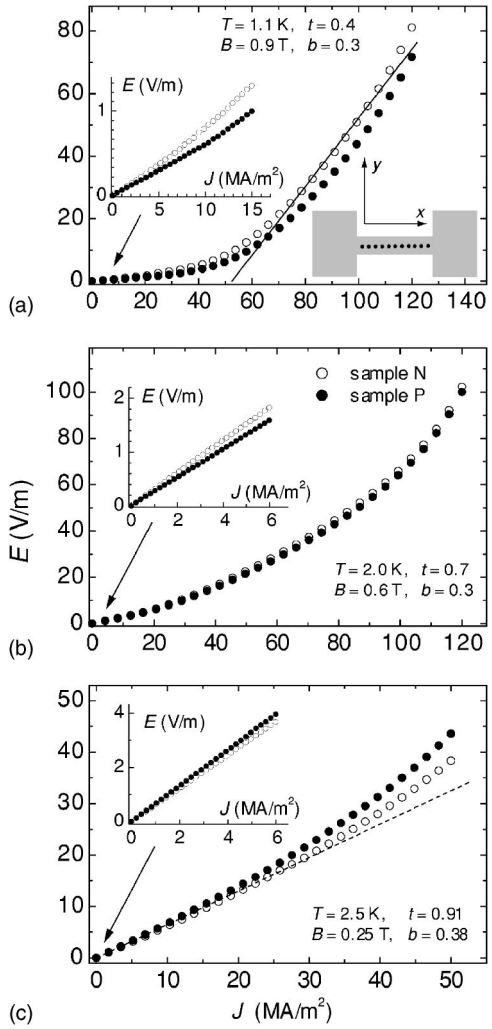

FIG. 1. $E(J)$ of sample N (○) and sample P (●) for (a) $T=1.1$ K, $B=0.9$ T, (b) $T=2.0$ K, $B=0.6$ T, and (c) $T=2.5$ K, $B=0.25$ T. The solid and dashed lines are plots of LO ρ_f expected at low and high t, respectively. Lower inset to (a): A sketch of sample P (not to scale) and the designation of the directions (see the text). Upper inset to (a) and insets to (b), (c): The initial parts of the $E(J)$ in an expanded scale for a better view.

the same Si/SiO_2 substrate as described in Ref. 10. One of the samples (sample P) was perforated with a line of equidistant holes along the central axis of the microbridge (designated as x direction) as sketched in the lower inset to Fig. 1(a). The holes had a diameter of 800 nm [slightly smaller than $\lambda(0)$] and their center-to-center distance was 1.2 μm. Both samples had the same $T_c=2.75$ K and the same overall normal-state and superconducting properties. Throughout the paper we use the nonperforated sample (sample N) as a reference for identifying the effects of holes. Its transport properties were analyzed in detail in Ref. 11, and its GL parameters $\xi(0)=6.8$ nm and $\lambda(0)=1.15$ μm are taken as representative of both samples.

The measurements were carried out in a ^{3}He system equipped with a commercial calibrated superconducting magnet and homemade rf filtering of measurement leads. A magnetic field was applied perpendicularly to the film plane and a dc current was passed in the x direction, so that the vortices traversed the sample in the y direction. The applied-current sweep rate was found not to affect the measured $E(J)$ up to at least 50 nA/s, and the rate used in the presented measurements was 10 nA/s. The applied current is for sample P converted into the *average* current density J_P by calculating the (uniform) current density J_N for sample N and taking the ratio of the normal-state resistances to determine $J_P=1.23J_N$. We use this notation, together with E_N, E_P for the electric field in samples N and P, respectively, when referring to the $E(J)$ of the two samples specifically. At high J the $E(J)$ exhibit nonlinearities due to the flux-flow instabilities that are related to the nonequilibrium changes of vortex cores.[11] Here we concentrate on the close-to-equilibrium regime where these effects have not yet been developed and the vortex cores maintain their equilibrium properties.

In order to investigate whether the differences in the $E(J)$ of the two samples could originate from, e.g., small variations of T and/or B, at several (B,T) points we checked reproducibility of our measurements. In all cases the reproducibility of the measured voltage was within 0.5%, which allowed us to identify the differences between $E_N(J_N)$ and $E_P(J_P)$ reliably. Moreover, the behavior presented below was also found in a less detailed set of measurements on another pair of samples, of which one was nonperforated and one with a less dense line of (not equidistant) holes of the same diameter.

In Fig. 1 we plot typical $E(J)$ representative of three temperature regimes: (a) T well below T_c (1.1 K, $t=0.4$), (b) intermediate t (2.0 K, $t=0.7$), (c) T close to T_c (2.5 K, $t=0.91$). The open circles show $E_N(J_N)$, solid circles $E_P(J_P)$, and the lines different theoretical predictions of the Larkin-Ovchinnikov (LO) flux flow (FF) theory,[12] as discussed below. The scaled magnetic field $b=B/B_{c2}$ corresponds to 0.30–0.38, the B_{c2} values being (a) 3.0, (b) 2.0, and (c) 0.65 T, with the uncertainty of around 5%. At low T [Fig. 1(a)] the $E(J)$ of both samples reveal two different dynamic regimes: thermally activated magnetoresistance at $J\to 0$, followed at larger J by an $E\propto(J-J_c)$ behavior that implies FF against a background pinning potential with a depinning threshold J_c.[10] The solid line is a plot of the latter dependence, with the slope $dE/dJ=\rho_n b/0.9$ equal to the low-t LO FF resistivity ρ_f (ρ_n is the normal-state resistivity), and J_c chosen to obtain a fit to $E_N(J_N)$. The LO theory describes this part of $E(J)$ reasonably well until the out-of-equilibrium nonlinearities in $E(J)$ start to take place at large J.[11] As can be seen, the power dissipation in sample P is lower for $\sim$10% throughout the whole current-density range, suggesting an efficient pinning by the holes even far below T_c. In Fig. 1(b) we show the $E(J)$ at $T=2.0$ K ($t=0.7$), just at the boundary of the low-t and high-t regimes, displaying a weaker reduction of E_P below E_N. Close to T_c [Fig. 1(c)] the theoretical high-t LO ρ_f (see Ref. 11 for details), shown by the dashed line, describes $E_N(J_N)$ excellently starting from $J=0$ and up to the appearance of the nonlinearities mentioned before. However, over the entire current-density range the dissipation in sample P is larger than in sample N, unexpectedly and in contrast to the result at lower temperatures. The reason for this peculiar behavior cannot be found in the pinning properties of holes.

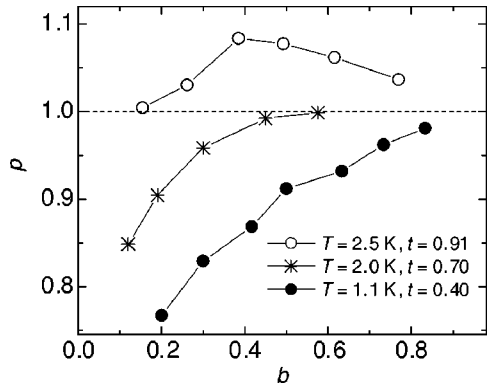

FIG. 2. The ratio $p=P_P/P_N$ of the power dissipated in samples P and N, integrated up to the appearance of the flux flow instabilities, vs $b=B/B_{c2}$. Sufficiently below T_c the holes reduce the dissipation ($p<1$) whereas close to T_c the situation is opposite.

The magnetic field range over which $E_N \neq E_P$ is wide at all three characteristic temperatures. This is demonstrated in Fig. 2, where we plot the ratio $p=P_P/P_N$ of the power density dissipated in samples P and N vs $b=B/B_{c2}$. The integration $P_{N,P}=\int E_{N,P}dJ_{N,P}$ is for each curve performed over the maximum region where the dissipation is not affected by the FF instabilities. We checked whether p depends on the upper limit of integration, and we found minor numerical differences of the order of 10–15 % of the values shown in Fig. 2, with no change in the general shape of $p(b)$. As can be anticipated from the $E(J)$ shown in Figs. 1(a) and 1(b), for $t=0.4$ and $t=0.7$ we find $p<1$, i.e., the holes are active pinning sites and decrease the dissipation. Their relative contribution to the pinning becomes smaller as t and b increase, which is expected qualitatively and discussed in the next Section. Close to T_c the dissipation in sample P is always larger, thus $p>1$ with a maximum around $b\sim 0.4$. This enhancement implies a suppression of the artificial pinning by another effect which is fully manifested close to T_c.

III. DISCUSSION

In order to understand the above results one has to address the equation of motion for the vortices

$$m\dot{\mathbf{u}} = \mathbf{F}_d - \eta\mathbf{u} + \mathbf{F}_h + \sum_n \mathbf{F}_n, \qquad (1)$$

where $\mathbf{u}$ is the vortex velocity, η the vortex-motion viscosity, m the effective vortex mass per unit length,[13] $\mathbf{F}_d=\phi_0\mathbf{J}\times\hat{\mathbf{z}}$ the driving force ($\hat{\mathbf{z}}$ is the unit vector in the direction of the applied magnetic field), $\mathbf{F}_h$ the repulsive force between the mobile vortices and those pinned by the holes, and $\mathbf{F}_n$ representing other relevant forces (e.g., the interaction of mobile vortices with each other or with intrinsic pinning potential). The spatial dependence of the ith component of the vortex acceleration $\dot{\mathbf{u}}$ is given by $\dot{u}_i=\mathbf{u}\cdot\nabla u_i$. By solving Eq. (1) one finds the vortex-velocity profile $\mathbf{u}(\mathbf{r})$. The generated electric field, the x component of which contributes to measured E_P, is calculated as $\mathbf{E}(\mathbf{r})=\mathbf{u}(\mathbf{r})\times\mathbf{B}(\mathbf{r})$, where $\mathbf{B}(\mathbf{r})$ is related to the local vortex density $n(\mathbf{r})=B(\mathbf{r})/\phi_0$.

The procedure just outlined in principle requires a knowledge of the details of $\mathbf{F}_h$ and $\mathbf{F}_n$—which depend on the superconducting properties, as well as the inhomogeneous profile of $\mathbf{J}$. However, for qualitative reasoning one can take into account the known characteristics of the vortex state in a particular (B,T) point to simplify the right-hand side of Eq. (1) by keeping the most relevant terms only.

In the spirit of such an approach we first discuss the role of $\mathbf{F}_h$. When confining a pinned vortex each hole acts as a source of repulsion to other vortices, with $\mathbf{F}_h$ pointing radially from the center of the hole. The repulsive force between two vortices separated by $r\ll\lambda$ is proportional to $\lambda^{-2}\ln(\lambda/r)$ and therefore weakens as $\lambda\to\infty$. Furthermore, the probability of a vortex being pinned by a hole becomes progressively smaller as λ grows much larger than the hole diameter.[8] Hence it is reasonable to assume that $\mathbf{F}_h$ decreases monotonically with increasing λ and eventually becomes irrelevant in the limit of diverging λ at $T\to T_c$. This leads to a plausible assumption that close to T_c even a very weak $\mathbf{J}$ may result in $\mathbf{F}_d\gg\mathbf{F}_h$.

Of the terms $\mathbf{F}_n$ the dominant ones are most likely those which account for the vortex interaction with the background pinning, and for the stiffness of the vortex lattice expressed through the shear-stress modulus C_{66}. The former contibution vanishes at the irreversibility field $B_{\rm irr}$ irrespective of its nature (i.e., vortex-lattice melting or depinning), whereas C_{66} drops discontinously to zero at the melting field B_m. It is known that $B_{\rm irr}$ in amorphous Nb–Ge films is rather low[10,11,14] and that it may be close to the melting field calculated theoretically.[15] The agreement of ρ_f and $E_N(J_N)$ at $t=0.91$ [Fig. 1(c); see also Ref. 11] down to the lowest B under consideration implies $B_{\rm irr}(t=0.91)<B$ for these results. Although the $B_{\rm irr}$ cannot be interpreted with certainty as the B_m, since $C_{66}\propto U_c(t)$ is close to T_c small,[16] $\mathbf{F}_d$ can easily overcome the long-range vortex-vortex interactions. Together with the smallness of $\mathbf{F}_h$, only the term $\mathbf{F}_d$ on the right-hand side of Eq. (1) remains relevant in the limit $T\lesssim T_c$. Thus we use this (independent-vortex) approximation to discuss the dissipation enhancement by the perforation close to T_c, as follows.

The driving force $\mathbf{F}_d$ is not uniform around the holes because the supercurrent density $\mathbf{J}$ is spatially modulated. A schematic of the modulation of $\mathbf{J}$, and consequently of $\mathbf{F}_d$, around the holes is shown in Figs. 3(a) and 3(b) by the dashed lines. In the regions denoted by H the driving force is larger than far from the holes, while in the regions denoted by L the situation is the reverse. Assuming negligible $\mathbf{F}_h$ and $\mathbf{F}_n$ in the vicinity of T_c, as discussed above, the vortices are accelerated parallel to $\mathbf{F}_d$ (perpendicular to $\mathbf{J}$), thus the vortex trajectories accumulate in regions H as sketched in Fig. 3(a) by the solid lines. The second effect of the current modulation is that in regions H the vortices move faster than in the sample bulk and produce a larger local electric field, while in regions L the opposite happens. Although the holes themselves shorten the distance the fast vortices travel in regions H, a sufficient imbalance in favor of the number of these vortices, together with their large acceleration, may result in the total dissipation in sample P being larger than in sample N. Therefore if a highly dense two-dimensional array

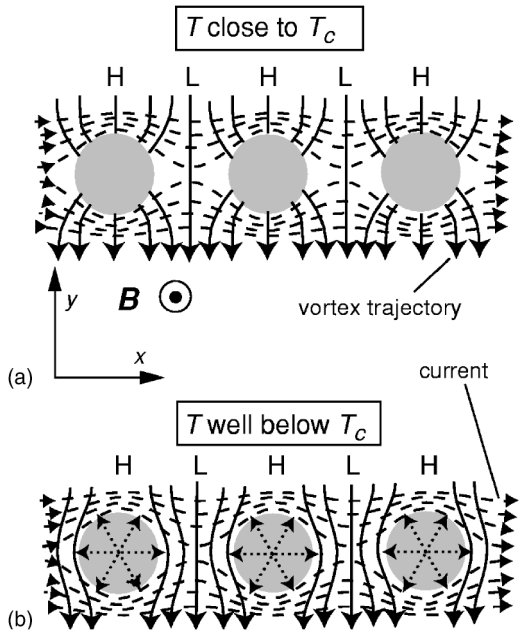

FIG. 3. A qualitative consideration of the vortex trajectories (arrowed solid lines) around the holes at (a) T close to T_c and (b) T well below T_c. The modulated current is indicated by the arrowed dashed lines, the density of which represents the magnitude of J. Arrowed dotted lines in (b) depict the repulsion excerted by the vortices pinned by the holes upon the other vortices. The labels L and H denote regions of low and high vortex flow density, respectively.

of holes[17] is intended to be used for enhancing the pinning of a sample there is no guarantee that this will work close to T_c in the presence of a transport current, although the magnetization loops may widen up. Moreover, the current-induced vortex-velocity enhancement strengthens with increasing J, which sheds more light on the similar result of Ref. 7 which also occurred at a relatively large applied current.

The nonmonotonic b dependence of $p>1$ may be linked to the competition between the enhanced current drive around the holes and the mutual repulsion of the mobile vortices, as explained below. The excess electric field relative to that far from the holes is estimated as $\Delta E \sim \phi_0 \Delta u \Delta n$, where Δu and Δn are the effective excess vortex velocity and density in regions H, respectively. While Δu depends on $\mathbf{J}$, η, m, and is independent of B, Δn also depends on the repulsive interaction between the mobile vortices, which is weak at low b and strong at high b. At low fraction $b=B/B_{c2}$ of the volume filled with the vortices they can all easily be channeled through regions H. Thus a larger vortex density results in the larger Δn and ΔE. On the other hand, Δn is at high b limited by the reduced space available for the channeling, which decreases ΔE and in turn results in a nonmonotonic $p(b)$.

As temperature is lowered λ becomes smaller and the holes start to pin more efficiently,[8] which explains qualitatively the stronger reduction of the dissipation at lower temperatures (Fig. 2). The vortices trapped by the holes now repel the incoming vortices and change the vortex trajectories depicted in Fig. 3(a) to those shown in Fig. 3(b). The repulsive force $\mathbf{F}_h$ is indicated by the dotted arrows. In a simple model of pinning by the holes in dynamic conditions a vortex remains pinned by a hole for some time until it is replaced by an incoming vortex. At low vortex density almost all vortices in the vicinity of holes are either pinned by them or scattered to pass through regions L of low current density. Hence the holes cause a noticeable reduction of the dissipation. As B increases the incoming vortices exert more force upon those pinned at the holes, reduce the pinning time, and the overall suppression of the dissipation decreases. This qualitative picture may explain the behavior of $p(b)$ at low temperatures.

We note, however, that the above explanation is still based on the single-vortex approximation, which disregards the enhanced stiffness of the vortex lattice far below T_c. The primary consequence of such a collective effect is expected to be an increase of J_c by the holes. Indeed, for $J>J_c$ in Fig. 1(a) $E_P(J_P)$ is essentially shifted with respect to $E_N(J_N)$, having nearly the same slope, which supports this expectation. Thus, although the single-vortex approximation of Eq. (1) suffices for a qualitative explanation of the low-temperature pinning by the holes, a more quantitative approach should include the long-range vortex-vortex correlations as well.

IV. SUMMARY AND CONCLUSIONS

In conclusion, we have patterned a line of holes with a diameter close to $\lambda(0)$ along an amorphous $Nb_{0.7}Ge_{0.3}$ microbridge. A comparison of the measured $E(J)$ curves of the samples with and without perforation reveals an unusual crossover in the power dissipation close to and well below T_c. Close to T_c the artificial pinning is weak and an unexpected rise of the dissipation is observed. This is attributed to the inhomogeneous current distribution around the holes leading to a significant increase of the local vortex velocity. As temperature is lowered the pinning by the holes becomes stronger and eventually suppresses the vortex velocity enhancement. In addition, our weak background pinning has permitted, to our knowledge, the first observation the pinning properties of holes as artificial pinning centers far below T_c.

ACKNOWLEDGMENTS

We thank B. Stojetz, A. Bauer, F. Rohlfing, W. Meindl, and M. Furthmeier for their technical assistance. This work was partly funded by the Deutsche Forschungsgemeinschaft within the Graduiertenkolleg 638. We gratefully acknowledge additional support by the Croatian Ministry of Science (Project No. 119262) and the Bavarian Ministry for Science, Research and Art.

*Electronic address: dbabic@phy.hr

[1] O. Daldini, P. Martinoli, J. L. Olsen, and G. Berner, Phys. Rev. Lett. **32**, 218 (1974); A. T. Fiory, A. F. Hebard, and S. Somekh, Appl. Phys. Lett. **32**, 73 (1978).

[2] M. Baert, V. V. Metlushko, R. Jonckheere, V. V. Moshchalkov, and Y. Bruynseraede, Phys. Rev. Lett. **74**, 3269 (1995); V. V. Moshchalkov, M. Baert, V. V. Metlushko, E. Rosseel, M. J. Van Bael, K. Temst, R. Jonckheere, and Y. Bruynseraede, Phys. Rev. B **54**, 7385 (1998).

[3] T. Matsuda, K. Harada, H. Kasai, O. Kamimura, A. Tonomura, and V. V. Moshchalkov, Science **271**, 1393 (1996).

[4] J. I. Martin, M. Veléz, J. Nogués, and I. K. Schuller, Phys. Rev. Lett. **79**, 1929 (1997).

[5] M. Velez, D. Jaque, J. I. Martin, M. I. Montero, I. K. Schuller, and J. L. Vicent, Phys. Rev. B **65**, 104511 (2002).

[6] D. Jaque, E. M. González, J. I. Martin, J. V. Anguita, and J. L. Vicent, Appl. Phys. Lett. **81**, 2851 (2002).

[7] Z. Jiang, D. A. Dikin, V. Chandrasekhar, V. V. Metlushko, and V. V. Moshchalkov, cond-mat/0312508 (unpublished).

[8] N. Takezawa and K. Fukushima, Physica C **228**, 149 (1994).

[9] V. V. Moshchalkov, M. Baert, V. V. Metlushko, E. Rosseel, M. J. Van Bael, K. Temst, Y. Bruynseraede, and R. Jonckheere, Phys. Rev. B **57**, 3615 (1998).

[10] D. Babić, T. Nussbaumer, C. Strunk, C. Schönenberger, and C. Sürgers, Phys. Rev. B **66**, 014537 (2002).

[11] D. Babić, J. Bentner, C. Sürgers, and C. Strunk, Phys. Rev. B **69**, 092510 (2004).

[12] A. I. Larkin and Yu. N. Ovchinnikov, in *Nonequilibrium Superconductivity*, edited by D. N. Lengenberg and A. I. Larkin (North Holland, Amsterdam, 1986).

[13] See, e.g., E. M. Chudnovsky and A. B. Kuklov, Phys. Rev. Lett. **91**, 067004 (2003), and references therein.

[14] J. M. E. Geers, C. Attanasio, M. B. S. Hesselberth, J. Aarts, and P. H. Kes, Phys. Rev. B **63**, 094511 (2001).

[15] G. Blatter, B. Ivlev, Y. Kagan, M. Theunissen, Y. Volokitin, and P. Kes, Phys. Rev. B **50**, 13013 (1994).

[16] E. H. Brandt, Phys. Rev. B **34**, 6514 (1986).

[17] U. Welp, Z. L. Xiao, J. S. Jiang, V. K. Vlasko-Vlasov, S. D. Bader, G. W. Crabtree, J. Liang, H. Chik, and J. M. Xu, Phys. Rev. B **66**, 212507 (2002).